

## Analysis of Spectra from Laser Produced Plasmas Using a Neural Network

A. L. Osterheld,<sup>1</sup> W. L. Morgan,<sup>2</sup> J. T. Larsen,<sup>3</sup> B. K. F. Young,<sup>1</sup> and W. H. Goldstein<sup>1</sup>

<sup>1</sup>Lawrence Livermore National Laboratory, University of California, P.O. Box 808, Livermore, California 94550

<sup>2</sup>Kinema Research, P.O. Box 1147, Monument, Colorado 80132

<sup>3</sup>Cascade Applied Sciences, Inc., P.O. Box 4477, Boulder, Colorado 80306

(Received 20 December 1993)

A backpropagation artificial neural network algorithm is applied to the analysis of *K*-shell x-ray line spectra from a well characterized laser produced plasma. After training on synthetic spectra produced by appropriate collisional radiative plasma emission models, the network correctly determines the electron temperature as a function of distance into the plasma. The results demonstrate the potential utility of neural networks for interpreting spectral data from plasma devices and sources.

PACS numbers: 52.70.La

Artificial neural networks [1,2] are expected to be useful in applications involving the inversion of observational data to obtain physical quantities [3,4]. The procedure can be viewed as analogous to pattern recognition, for which neural networks are known to be well suited. A variety of problems in areas as diverse as transport [4], molecular physics [5], geophysics [6], chemical reaction kinetics [7], atomic level classification [8], and infrared spectroscopy [9,10] have been successfully cast as pattern recognition problems and addressed with neural networks. We explore here the application of neural network algorithms to inverting the relationship between measured plasma emission spectra and the plasma conditions that produce them.

Emission spectroscopy has long been the standard technique [10,11] for finding the temperature and density of high temperature plasmas, such as those found in astrophysical objects, in laboratory magnetically or inertially confined fusion plasmas, and in partially ionized laboratory plasmas, such as lighting or plasma processing discharges. One measures the peak intensities, and perhaps the widths, of a number of spectral lines being emitted by the plasma and compares the results with model calculations in order to deduce  $T_e$  and  $N_e$ , the electron temperature and density. Typically, certain spectral lines will be brighter at certain temperatures and densities and other lines will dominate in other regions of  $T_e$  and  $N_e$ . Temperature sensitivity, for example, is seen in the relative intensities of transitions with different energy thresholds, such as lines from different shells or charge states or resonance to satellite transitions. Density sensitivity arises from collisional quenching of excited states and can be seen in forbidden transitions or transitions from different atomic shells in a recombining plasma. For a given temperature and density relative ionization fractions are revealed in the intensities of transitions in different ionization states. The general principle is that examination of enough lines will give a unique estimate of temperature, density, and charge state.

The models used in plasma spectroscopy may be fairly simple, such as the limiting cases of local thermodynamic equilibrium or coronal equilibrium, or they may

be quite complex collisional radiative models possibly even including hydrodynamics. The process of modifying parameters in such models, performing the collisional radiative calculations, generating synthetic spectra, and comparing with the measured spectra, takes considerable effort and time. The analysis is typically hampered by noisy and incomplete data and by theoretical uncertainties in the models. In this paper we present plasma spectroscopic analysis of a laser produced plasma performed using a neural network that has been trained on detailed collisional radiative models. The concept that we are exploring is that this approach to plasma spectroscopy may potentially be able to simplify and make more robust the analysis process and, perhaps, automate it as part of an expert system. Although we have been developing the neural net techniques using simple *K*-shell spectra, the ultimate goal is to take advantage of the abilities of neural networks to assimilate large amounts of input information in order to infer plasma conditions from complex spectra.

Artificial neural networks consist of layers of simulated "neurons" with associated activation functions, transfer functions, and weighting functions for the "synapse" connections to other neurons. The key elements are an input layer of neurons, one or more "hidden" layers, and an output layer. Each neuron has a transfer or response function associated with it, typically the logistic function  $T(x) = 1/(1 + e^{-x})$ , that gives an output value that is a nonlinear function of the sum of the input values. The input values are the weighted outputs of each neuron in the previous layer. That is, if the output of neuron  $j$  is  $o_j$  and  $w_{ij}$  is the weight connecting neurons  $i$  and  $j$ , then the output of neuron  $i$  is

$$o_i = T\left(\sum_j w_{ij}o_j\right) = 1 / \left(1 + e^{-\sum_j w_{ij}o_j}\right),$$

where the sum is over all neurons  $j$  having outputs that feed into neuron  $i$ . The hidden layers give the network a high degree of nonlinearity and, from the point of view of the network as a pattern matcher, provide an internal representation of the correlation between the input and

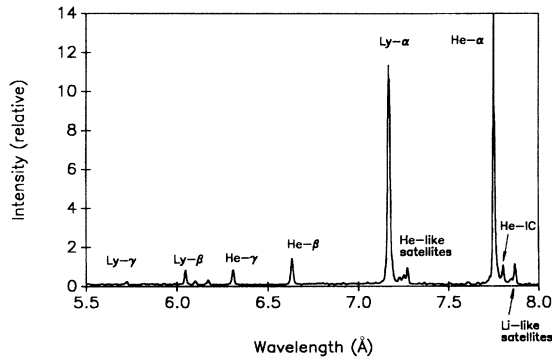


FIG. 1. *K*-shell spectrum from highly ionized aluminum showing the H- and He-like aluminum resonance lines, the He-like intercombination line, and the He- and Li-like Al satellite lines.

the output patterns. The network is “trained” by running a number of cases of known {input, target output} sets through it and adjusting the weights to minimize the sum of the squares of the differences between the desired result and the computed result. During this supervised learning process the neural network will assimilate and correlate data given it so that when given input vectors outside of the training set it will produce reasonable values for the corresponding output vectors. The matrix of weights  $w_{ij}$  represents the mapping between the set of input vectors and the set of output vectors and contains all the information correlating the output to the input. Because of the high degree of connectivity between the elements and comprising the network and their nonlinear response, neural networks have a generalization ability and are able to deal with noisy or even missing data. Because plasma x-ray spectra are frequently corrupted by noise and limitations on dynamic range, and because models carry their own uncertainties, these properties of neural networks are especially appealing for spectral analysis.

The x-ray spectra being analyzed were produced by a simple  $60 \times 52 \mu\text{m}$  aluminum dot target on a thick CH substrate that was irradiated by a 1.3 ns,  $7.35 \times 10^{13}$  W/cm<sup>2</sup> green laser pulse. Such microdot targets produce a nearly one-dimensional plasma with reduced opacity problems, especially for the late-time, relatively low-density corona. The x-ray spectrum consists primarily of hydrogenlike Al XIII and heliumlike Al XII lines and their satellites. A sample *K*-shell spectrum is shown in Fig. 1. Time and space resolving spectrometers recorded x-ray spectra from the aluminum in the 5–8 Å spectral region. These measurements are similar to those described in Refs. [12] and [13].

The plasma was modeled using a collisional radiative atomic physics model [13] of aluminum comprising a detailed description of the important low lying ionic levels plus an average model for the higher lying states. The atomic structure calculations were performed using

the Hebrew University–Lawrence Livermore atomic code (HULLAC). The energy levels and all important radiative transitions and autoionization rates were calculated using a relativistic, multiconfiguration parametric potential model [14]. All electron impact transitions between these levels were calculated in the quasirelativistic, distorted wave approximation [15]. These detailed components of the model were merged with an average level model constructed from single particle energies and transition rates [16]. Photoionization and recombination were based on subshell Hartree-Slater ionization cross sections [17] and the cross sections for collisional ionization and its inverse were obtained from Ref. [18]. Dielectronic recombination and excitation autoionization were included by explicitly treating the  $2lnl'$  and  $1s2nl'$  levels for  $n \leq 4$ , and by implicitly including these processes in the isolated resonance approximation using configuration averaged autoionization rates [19] for  $5 \leq n \leq 10$ .

The conventional modeling procedure [13] used to extract plasma conditions and charge state abundances consists of solving the collisional radiative rate equations, generating synthetic spectra, and fitting to a measured spectrum using a least-squares exhaustive search minimization algorithm. The aluminum transitions used in this analysis include the hydrogenlike  $1s-np(^2P)$  and heliumlike  $1s^2-1snp(^1P_1)$  resonance lines for  $n \leq 5$ , and the heliumlike  $1s^2-1s2p(^3P_1)$  intercombination (IC) line. In addition, the heliumlike  $1s2l-2l2l'$  and lithiumlike  $1s^22l-1s2l2l'$  satellite transitions [20] were included in the modeling. These transitions have been widely used to diagnose hot plasmas using both steady-state and quasi-steady-state approximations [13,20–22]. They have previously been shown to determine plasma conditions that agree with direct free-bound recombination continuum temperature and interferometric density measurements in the same plasma analyzed here [22,23]. The quasi-steady-state model allows a nonequilibrium ionization distribution but assumes the excited populations are in steady state due to the rapid time scale for excited-state equilibration [21]. The plasma studied here is nearly in steady-state equilibrium in the dense region near the target surface. In the expanding, cooling plasma at large distances from the target surface the plasma is overionized and recombining [13]. As shown in Fig. 2 both models yield the same temperatures out to about  $80 \mu\text{m}$  into the plume but diverge in their predictions at greater distances from the target.

We examined three neural network configurations in this study. In each case the networks were trained on 200 simulated spectra until the output neurons were matched to an accuracy of 10% for electron temperature, 20% for electron density, and (for the third network) 10% for the average  $Z$  (ionization state) of the plasma. Gaussian noise at the 10% level was added to the simulated spectra on each training iteration. The parameters of the synthetic spectra ranged from 200 to 1200 eV, from  $10^{20}$  to

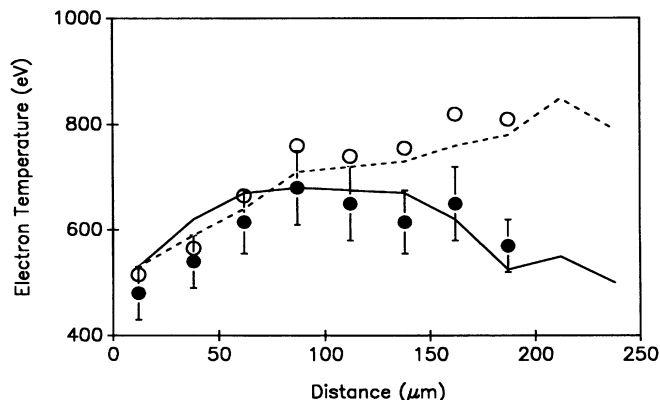


FIG. 2. Plasma temperature versus distance from the target as predicted by various procedures: (---) conventional plasma spectroscopic technique using steady-state model; (—) conventional technique using quasi-steady-state model; (○) neural network trained on steady-state model; and (●) neural network trained on quasi-steady-state model.

$10^{21} \text{ cm}^{-3}$ , and (for the third case) from Li-like to fully ionized. These span the range of expected values for the spectra treated here. A universal network spanning the range of conditions where these aluminum transitions have diagnostic applications would require a larger number of training spectra.

In the first instance the network was trained on simulated spectra consisting of H-like and He-like aluminum resonance lines for principal quantum number  $n \leq 5$  and the He-like intercombination line; nine transitions in all. These spectra were obtained from a steady-state collisional radiative equilibrium model. The network thus consisted of a nine neuron input layer where each neuron represents the relative intensity of one of the nine x-ray lines, two hidden layers each having fifteen neurons, and an output layer having three neurons representing  $T_e$ ,  $N_e$ , and  $\bar{Z}$ , respectively. The second configuration that we examined also had two fifteen neuron hidden layers and was trained on steady-state simulated spectra comprising H- and He-like resonance lines with  $n \leq 4$ , the He-like IC line, three He-like satellite lines, and one Li-like satellite; eleven lines in all. The third neural network configuration comprised two hidden layers of seventeen neurons each and was trained on simulated spectra generated with a quasi-steady-state model using the same spectral features as in the second case.

Each of the three network configurations was applied, after training, to the space and time resolved spectra taken in the laser produced plasma experiment. The first network, which included only resonance transitions, correctly reproduced the electron temperature near the target surface but gave oscillatory results when applied to spectra from the recombining plasma farther from the target. This is because the resonance lines alone do not accurately reflect the electron temperature in a

recombining plasma. The second neural net configuration included satellite transitions, which are clearly seen in the spectra taken of the plume region of the plasma. The intensities of satellite transitions relative to their parent resonance lines are a more robust diagnostic of the electron temperature in transient plasmas [21]. As shown in Fig. 2, this network accurately reproduced the results obtained from a conventional steady-state analysis. This, however, leads to an overestimate of the electron temperature in the recombining plume region of the plasma because the plasma is overionized in this region. In order to match the relative intensities of the H-like transitions compared to the He-like transitions in the plume a steady-state model requires a temperature substantially higher than the true temperature. In the third network the steady-state constraint is relaxed and the charge state distribution is treated as a parameter independent of  $T_e$  and  $N_e$ . As shown in Fig. 2, the network accurately reproduces the electron temperatures in both the steady-state region and the recombining regions of the plasma.

Essentially all of the computational effort of the neural network approach to spectral interpretation is in the training phase. In the present examples the quasi-steady-state network takes several times as long to train as the other two networks. This is because the sensitivity of the spectra to the temperature and density can be partially masked by changes in the ionization balance, if the steady-state constraint is removed. This training time is equivalent to the time required to interpret a few hundred spectra using the conventional method. However, once trained, the neural networks interpret spectra much more rapidly than the conventional least-squares technique. This is because the least-squares method must iteratively solve a set of linearized equations, while the neural network interprets the spectra by a few simple algebraic computations using the predetermined weights. The neural network distills the spectral dependencies from complex plasma emission calculations into "formulas" for the output parameters. Thus, the "cost" of training the network is rapidly amortized, and the results of theoretical calculations may easily be transferred to the many experimental groups using spectral diagnostics, even for quasi-steady-state diagnostics which defy simple tabular description.

We have demonstrated that neural network algorithms work well for obtaining plasma conditions from the fairly simple K-shell aluminum x-ray spectrum. Although the simple K-shell spectrum analyzed was tractable by standard exhaustive search techniques, as Jeffrey and Rosner point out [3], the fitting of complex emission and absorption line spectra by exhaustive search can be prohibitive. We have chosen a small number of well defined lines for examination but the neural net algorithm should be capable of working with a raw spectrum. It would correlate features in a synthetic spectrum with features in the measured spectrum even if there is some

uncertainty in the position of the lines as well as noise affecting the intensity of the lines. In such a scheme the information contained in the linewidths could also be used to aid in characterizing the plasma properties. One could, in principle, construct a library of neural network weight matrices based on learning the synthetic spectra computing using very sophisticated and computationally intensive collisional radiative models. This library could then be accessed by neural network programs performing the plasma spectroscopic analysis.

This work was performed under the auspices of the U.S. Department of Energy by LLNL under Contract No. W-7405-Eng-48.

- 
- [1] J. Hertz, A. Krogh, and R.G. Palmer, *Introduction to the Theory of Neural Computation* (Addison-Wesley, Redwood City, CA, 1991).
- [2] P.D. Wasserman, *Neural Computing* (Von Nostrand Reinhold, New York, 1989).
- [3] W. Jeffrey and R. Rossner, *Astrophys. J.* **310**, 473 (1986).
- [4] W.L. Morgan, *IEEE Trans. Plasma Sci.* **19**, 250 (1991).
- [5] B.G. Sumpter, C. Getino, and D.W. Noid, *J. Chem. Phys.* **97**, 293 (1992).
- [6] H. Lundstedt, *Planet. Space Sci.* **40**, 457 (1992).
- [7] N.V. Bhat, P.A. Minderman, Jr., T. McAvoy, and N. Sun Wang, *IEEE Control Systems Magazine* (April 1990), p. 24.
- [8] K.L. Peterson, *Phys. Rev. A* **41**, 2457 (1990).
- [9] K. Tanabe, T. Tamura, and H. Uesaka, *Appl. Spectros.* **46**, 807 (1992).
- [10] H. Griem, *Plasma Spectroscopy* (McGraw-Hill, New York, 1964).
- [11] J. Cooper, *Rep. Prog. Phys.* **29**, 35 (1966).
- [12] B.K.F. Young, R.E. Stewart, C.J. Cerjan, G. Charatis, and Gar. E. Busch, *Phys. Rev. Lett.* **61**, 2851 (1988).
- [13] B.K.F. Young, W.H. Goldstein, A.L. Osterheld, R.E. Stewart, G. Charatis, and Gar. E. Busch, *J. Phys. B* **22**, L533 (1989).
- [14] M. Klapisch, *Comput. Phys. Commun.* **2**, 239 (1971); M. Klapisch, J.L. Schwob, B.S. Fraenkel, and J. Oreg, *J. Opt. Soc. Am.* **61**, 148 (1977).
- [15] A. Bar-Shalom, M. Klapisch, and J. Oreg, *Phys. Rev. A* **38**, 1773 (1988).
- [16] J.H. Scofield (unpublished).
- [17] J.H. Scofield (private communication); E.B. Saloman, J.H. Hubble, and J.H. Scofield, *At. Data Nucl. Data Tables* **38**, 1 (1988).
- [18] D.H. Sampson and L.B. Golden, *Astrophys. J.* **170**, 169 (1971); D.L. Moores, L.B. Golden, and D.H. Sampson, *J. Phys. B* **13**, 385 (1980).
- [19] M.H. Chen, *Phys. Rev. A* **40**, 2758 (1989).
- [20] A. Gabriel, *Mon. Not. R. Astron. Soc.* **160**, 99 (1972).
- [21] V.A. Boiko, I.Yu. Skobelev, and A.Ya. Faenov, *Sov. J. Plasma Phys.* **10**, 82 (1984).
- [22] A.L. Osterheld, B.K.F. Young, R.L. Shepherd, R.S. Walling, W.H. Goldstein, and R.E. Stewart, *Bull. Am. Phys. Soc.* **36**, 2432 (1991); (to be published).
- [23] B.K.F. Young, A.L. Osterheld, G.M. Shimkaveg, R.L. Shepherd, R.S. Walling, W.H. Goldstein, and R.E. Stewart, *J. Quant. Spectros. Radiat. Transfer* **51**, 417 (1994).